Urban Forestry & Urban Greening 112 (2025) 128997

Contents lists available at ScienceDirect

Urban Forestry & Urban Greening

journal homepage: www.elsevier.com/locate/ufug

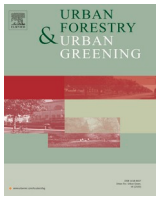

Original article

Urban green space classification using Object-Based Image Analysis (OBIA) and LiDAR fusion: Accuracy evaluation and landscape metrics assessment

Mika Siljander [a,e,*], Sameli Männistö [b], Kirsi Kuoppamäki [b,f], Maija Taka [c], Olli Ruth [d]

[a] Helsinki Lab of Interdisciplinary Conservation Science, Department of Geosciences and Geography, University of Helsinki, P.O. Box 64 FI-00014, Finland
[b] Faculty of Biological and Environmental Sciences, Ecosystems and Environment Research Programme, University of Helsinki, Niemenkatu 73, Lahti FIN-15140, Finland
[c] Water and Environmental Engineering Research Group, Aalto University, P.O. Box 15200, Espoo, Finland
[d] Department of Geosciences and Geography, University of Helsinki, P.O. Box 64 FI-00014, Finland
[e] Biodiversity Unit, University of Turku, Turku, Finland
[f] Lammi Biological Station, University of Helsinki, Pääjärventie 320, 16900 Lammi, Finland

ARTICLE INFO

Keywords:
Aerial photograph
FRAGSTATS
Green space
Landscape metrics
LiDAR point clouds
OBIA
Urban vegetation

ABSTRACT

With over two-thirds of the global population projected to live in cities by 2050, accurately mapping urban green spaces is increasingly important for sustainable development. This study integrates Object-Based Image Analysis (OBIA) and LiDAR data fusion to improve green space classification in three urban catchments in Helsinki, representing high (Itä-Pasila), intermediate (Pihlajamäki), and low (Veräjämäki) land-use intensities. Using high-resolution color-infrared (CIR) aerial orthophotographs enhanced by LiDAR-derived vegetation height data, the method effectively identified vegetated areas. Results were validated against a reference dataset using standard accuracy metrics and landscape structure indices. The results show that the OBIA method yielded green space area estimates within 1–4 % of the reference, but tended to produce more fragmented landscape configurations in high land-use intensity urban areas, resulting in higher numbers of patches and lower aggregation indices. Conversely, results in less urbanized Veräjämäki closely matched the reference data both spatially and structurally. These discrepancies underscore the inherent challenges in interpreting spatial patterns within complex urban morphologies, particularly where spectral information is limited by shading, like in Itä-Pasila. Nevertheless, the OBIA–LiDAR fusion approach demonstrated strong reliability in less structurally complex environments and provides valuable data for watershed-scale hydrological and ecological modeling.

1. Introduction

As global urbanisation accelerates, cities are increasingly confronted with environmental challenges that threaten both ecological balance and human well-being. Urban areas, which currently accommodate over half of the global population, are projected to host nearly 70 per cent by 2050 (United Nations, 2022). This rapid expansion often occurs at the expense of natural landscapes, as forests, wetlands, and vegetated surfaces are replaced by impervious structures such as roads, buildings, and car parks (Science, 2016). The ecological consequences of this transformation are substantial. Hydrological processes including infiltration and evapotranspiration are disrupted, resulting in increased surface runoff, reduced groundwater recharge, and a greater risk of flash flooding, particularly during extreme rainfall events intensified by climate change (Goldshleger et al., 2009; Pfleiderer et al.,2019). The substitution of vegetated areas with thermally absorptive built surfaces also contributes to the urban heat island effect, whereby urban areas experience significantly higher temperatures than their rural surroundings (Voogt and Oke, 2003). These changes negatively affect urban microclimates and are associated with increased public health risks, higher energy demand, and ecological degradation (Ward Thompson et al., 2012). Urban green infrastructure, including forests, parks, street trees, and green roofs, is increasingly recognised as a vital component of sustainable urban systems. Green spaces provide essential ecosystem services such as stormwater regulation, temperature moderation, carbon sequestration, air purification, and biodiversity support (Elmqvist et al., 2015; Gunawardena et al., 2017; Hidalgo García, 2023). However, the provision of these services is not solely dependent on the

* Corresponding author at: Helsinki Lab of Interdisciplinary Conservation Science, Department of Geosciences and Geography, University of Helsinki, P.O. Box 64 FI-00014, Finland.
E-mail address: mika.siljander@helsinki.fi (M. Siljander).

https://doi.org/10.1016/j.ufug.2025.128997
Received 30 October 2024; Received in revised form 24 June 2025; Accepted 6 August 2025
Available online 7 August 2025

presence of vegetation. Structural characteristics such as canopy height, layering, and spatial configuration significantly influence the capacity and distribution of ecosystem benefits (Lehmann et al., 2014; Alonzo et al., 2014; Ziter, 2016). For example, dense and tall canopies contribute more effectively to shading and evapotranspiration (Lehmann et al., 2014), while spatial connectivity between green patches facilitates wildlife movement and increases resilience to environmental stressors (Andersson et al., 2019). Despite this, urban vegetation is often fragmented, and its spatial configuration is frequently overlooked in both mapping and planning contexts (McGarigal et al., 2023; Derkzen et al., 2015).

Numerous remote sensing techniques have been developed for land use and land cover (LULC) mapping, including optical satellite imagery, Synthetic Aperture Radar (SAR), machine learning classifiers, deep learning approaches such as convolutional neural networks (CNNs) and U-Net architectures, as well as Object-Based Image Analysis (OBIA). These methods have been widely applied to capture spatial patterns and surface characteristics across diverse landscapes (Flanders et al., 2003; Xiaoxia et al., 2005; Zhang and Qiu, 2012; Zhou, 2013; Tong et al., 2014; Parmehr et al., 2016; Zhong et al., 2017; Georganos et al.,2018; Man et al., 2020; Megahed et al., 2021; Kuras et al., 2021; Shahtahmassebi et al., 2021; Jin and Mountrakis, 2022; Cheng et al., 2023). However, despite their success in general LULC delineation, these approaches often face limitations in complex urban environments. Issues such as spectral confusion from building shadows, overlapping land cover types, and heterogeneous surface materials frequently lead to misclassification (Lu and Weng, 2007; Myint et al., 2011; Yan et al., 2015). Traditional pixel-based classification methods, particularly when applied to very high-resolution imagery, tend to produce a 'salt-and-pepper' effect because of the lack of spatial context (Blaschke et al., 2000; Zhang and Qiu, 2012). To address these limitations, OBIA has been introduced as a more robust alternative by segmenting imagery into meaningful objects based on spectral, spatial, and contextual information (Blaschke, 2010). This approach improves classification accuracy by maintaining structural heterogeneity and facilitating the distinction between visually similar land cover types. OBIA also enables integration with auxiliary datasets such as airborne Light Detection and Ranging (LiDAR), which provides high-resolution three-dimensional structural information that is independent of lighting or spectral variability. LiDAR data allow for the extraction of ecologically relevant vegetation parameters, including canopy height, vertical stratification, and crown volume (Alonzo et al., 2014; Degerickx et al., 2020). When combined with OBIA, LiDAR significantly enhances the ability to classify structurally complex vegetation, including mid-storey and canopy trees, even in spectrally ambiguous urban zones. Despite these advantages, the combined application of OBIA and LiDAR in urban vegetation mapping remains underutilised (Blaschke et al., 2014; Degerickx et al., 2020). Many studies continue to rely on either spectral or structural data alone, thereby limiting their capacity to capture the full ecological complexity of green spaces (Mathieu et al., 2007; Gülçin and Akpınar, 2018). Furthermore, the spatial configuration of vegetation, which is essential for supporting ecological connectivity, mitigating thermal stress, and managing hydrological flows, is seldom quantified in a systematic manner (Zellweger et al., 2019).

Landscape metrics offer a means to address this gap. Quantitative indicators such as Patch Density, Largest Patch Index, Clumpiness, and Edge Density provide valuable insights into spatial structure and fragmentation, with direct implications for ecosystem functionality (McGarigal et al., 2023). However, such metrics have rarely been applied in urban vegetation studies using remote sensing data (Zhang and Qiu, 2012; Hu et al., 2022). This oversight is significant, as the spatial arrangement and connectivity of green spaces are key determinants of their effectiveness in providing cooling, stormwater retention, and habitat connectivity (Tzoulas et al., 2007). For instance, large, contiguous green patches are more effective in reducing urban temperatures and supporting biodiversity, whereas isolated or fragmented patches offer limited ecological value (Gill et al., 2007; La Rosa et al., 2014). Integrating landscape metrics into urban green space detection workflows links spatial patterns to ecological relevance.

This study addresses these methodological and conceptual gaps by developing a high-resolution urban vegetation classification framework that integrates OBIA-Lidar Fusion based green space mapping with landscape pattern analysis. The framework is applied to three catchments in Helsinki, Finland, which represent a gradient of urban form and vegetation complexity: Itä-Pasila (high land-use intensity), Pihlajamäki (intermediate land-use intensity), and Veräjämäki (low land-use intensity). These areas provide a robust testbed for evaluating classification performance across varied urban morphologies. The specific objectives of the study are: (i) to develop an integrated OBIA-based classification approach that fuses LiDAR and CIR data to map vegetated and non-vegetated surfaces, including vegetation height classes, at the catchment scale; (ii) to assess classification accuracy using traditional per-pixel validation metrics and spatial overlay comparisons with reference datasets; (iii) to quantify the spatial structure and fragmentation of green space and non-green areas using landscape metrics; and (iv) to evaluate the contribution of LiDAR-derived structural information in improving classification reliability, particularly in complex urban environments.

2. Materials and methods

2.1. Study sites

Three urban sub-catchments were selected in Helsinki, Finland (60°10′15″N, 24°56′15″E), to represent a gradient of urbanisation. The city has a cold continental climate, with four distinct seasons that influence vegetation dynamics. The study sites include Itä-Pasila (24.14 ha), Pihlajamäki (38.33 ha), and Veräjämäki (14.52 ha). Their locations and Land Cover / Land Use (LCLU) classifications, based on the Urban Atlas 2012 (European Environment Agency EEA.,2016), are shown in Fig. 1. The sites were previously included in a stormwater runoff and quality study conducted between September 2010 and September 2015 (Taka, 2012; Taka et al., 2017). Fig. 2 depicts color-infrared (CIR) orthophotographs and canopy height models (CHM) of the studied catchments.

Itä-Pasila is the most urbanised of the three. It consists largely of built surfaces, including buildings, roads, and parking lots, with limited and fragmented green space. Vegetation is restricted to small urban parks and street trees. Architecturally, the area reflects 1970s urban planning, with compact concrete structures and elevated decks. According to the Geological Survey of Finland (GTK, 2015), the superficial deposits consist mainly of exposed or shallow bedrock. Pihlajamäki, a residential district developed in the 1960s, contains more substantial green space interwoven with apartment blocks. The dominant soil type is clay, covering approximately 94.4 per cent of the catchment (15.4 km^2). Bedrock is present across 12.3 per cent of the area, while surface water covers less than 0.01 per cent. The low permeability of the clay soils limits infiltration and increases the importance of green infrastructure for runoff management. Veräjämäki, the least urbanised site, is characterised by detached housing and abundant green space. The southern part of the catchment contains extensive forest, while the northern part features private gardens. Bedrock is the principal superficial material, comprising 79.5 per cent of the area. Clay soils occupy 17.5 per cent, and surface water less than 0.02 per cent. This geological composition influences both vegetation patterns and drainage processes.

2.2. Remotely sensed data

2.2.1. Aerial images

This study employed very high-resolution red-green-blue (RGB) and color-infrared (CIR) orthophotos obtained from the City of Helsinki's geospatial repository. The CIR imagery included a near-infrared (NIR)

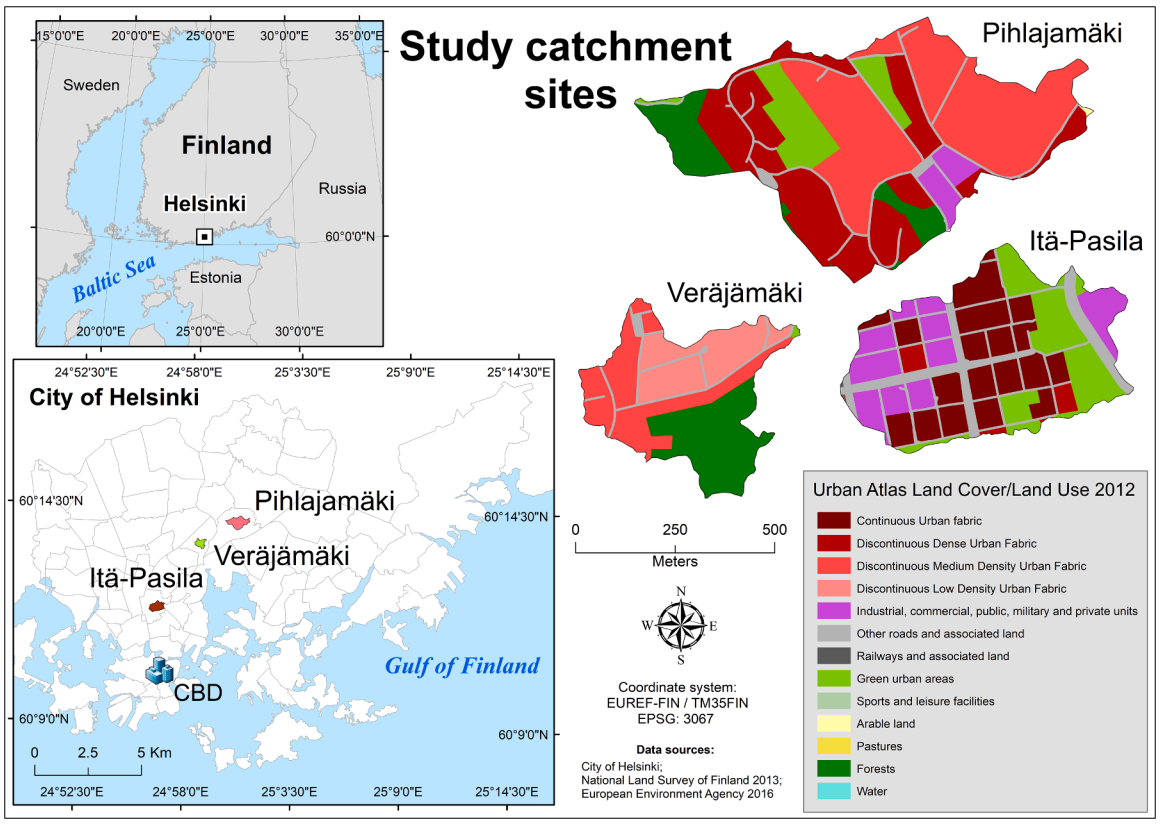

Fig. 1. Location of City of Helsinki with postal code areas and Central Business District (CBD). High (Itä-Pasila), intermediate (Pihlajamäki), and low (Veräjämäki) land-use intensity study catchment sites shown with Urban Atlas: Land Cover / Land Use Data for 2012 classes (Data sources: National Land Survey of Finland 2013; City of Helsinki; Urban Atlas: Land Cover / Land Use Data for 2012, European Environment Agency EEA, 2016).

band (800–900 nm), a green band (510–600 nm), and a red band (600–700 nm), with a ground resolution of 20 centimetres per pixel. The original orthophotos, captured during the City of Helsinki's aerial survey in June 2013, were mosaicked into a single continuous image. Subsequently, the composite image was masked and clipped according to the spatial extents of the delineated study catchments. CIR imagery was selected over RGB imagery due to its enhanced ability to distinguish vegetated areas. This advantage arises from the inclusion of the NIR band, which is strongly reflected by healthy vegetation owing to the internal leaf structure. As a result, CIR imagery offers superior contrast between vegetated and non-vegetated surfaces, facilitating more accurate segmentation and classification of vegetation cover (Gausman, 1977; Wolff et al., 2023; Zhao et al., 2024).

2.2.2. LiDAR data

In addition to aerial imagery, the classification process was enhanced through the integration of Light Detection and Ranging (LiDAR) data. The dataset was acquired by the National Land Survey of Finland (NLS) during a nationwide survey in 2008 and is part of the NLS open-access geospatial archives. The data were provided in LAS format and featured an average point density of 1.2 points per square metre. Prior to analysis, the LiDAR point cloud underwent preprocessing to improve data quality. This involved the automated detection and removal of outliers using the FilterData routine in the FUSION software package (version 4.61), a tool widely employed for LiDAR data processing in forestry and urban applications (McGaughey, 2024). Following this preprocessing step, the filtered point cloud was used to generate digital terrain models (DTMs) and to extract vegetation height information for land cover classification and structural analysis of green spaces.

2.3. Classification of vegetation

Vegetation classification was carried out using Object-Based Image Analysis (OBIA) within the Definiens eCognition Developer software (Trimble Geospatial, Munich, Germany). The initial step in this process involved segmentation, wherein pixels were automatically grouped into larger, more homogenous units known as objects. Segmentation was primarily driven by the color-infrared (CIR) data associated with each pixel. For this study, a multi-resolution segmentation approach was selected, as it allows for the local minimization of average heterogeneity within image objects at a given resolution. Users are required to specify a set of parameters for the segmentation, as detailed in the work of Zhou et al. (2009). The segmentation process was configured with a scale parameter of 60, a shape factor of 0.2, and a compactness factor of 0.5. A scale parameter of 60 was selected to yield an appropriate granularity for vegetation classification, balancing detail with generalisation. The shape factor was set to 0.2, thereby assigning greater weight to spectral properties, which was suitable given the spectral variability of the target vegetation classes. A compactness value of 0.5 provided a compromise between smooth object boundaries and the preservation of meaningful spatial structures, effectively reducing both over- and under-segmentation. These values were determined through iterative testing and visual evaluation to optimise object delineation, ensuring both spectral consistency and structural relevance. The segmentation process primarily utilised color-infrared (CIR) imagery as its spectral input. To identify vegetated surfaces, the Normalised Difference Vegetation Index (NDVI) (Rouse et al., 1973) was calculated for each object using Eq. 1:

$$NDVI = (NIR - RED) / (NIR + RED) \quad (1)$$

where, NIR and RED denote the near-infrared and red spectral bands.

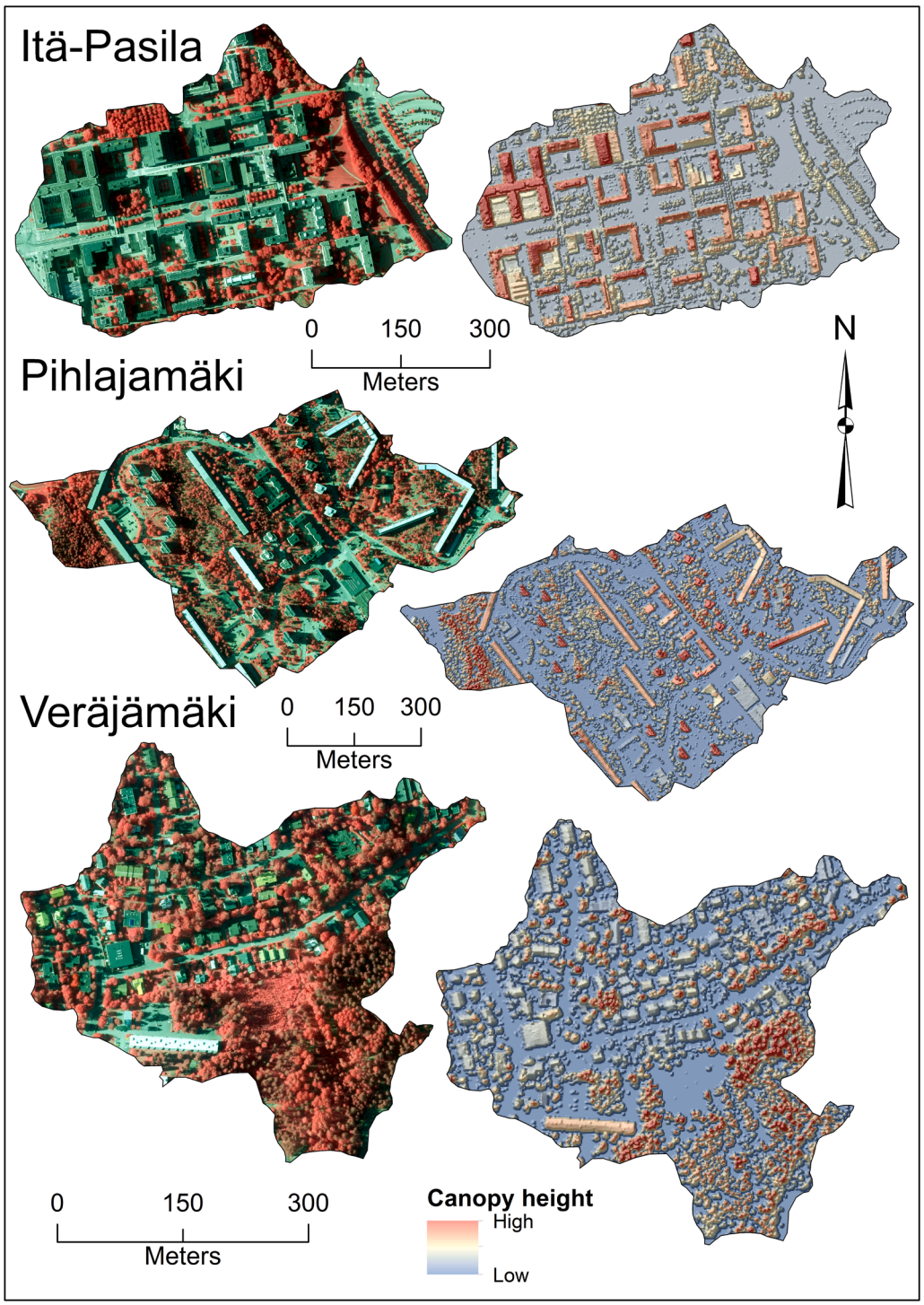

Fig. 2. Color-infrared (CIR) orthophotographs and canopy height models (CHM) of the studied catchments. Here CHM depicts all the objects in the area, including vegetation, buildings, and ground topography (Data sources: color-infrared (CIR) photos, City of Helsinki, 2013; LiDAR data, National Land Survey of Finland, 2013).

An NDVI threshold of 0.1 was adopted to distinguish vegetated areas (NDVI > 0.1) from non-vegetated surfaces (NDVI ≤ 0.1). This threshold is supported by both empirical studies and field observations, which demonstrate that impervious surfaces typically yield NDVI values below approximately 0.01 (occasionally up to 0.1), while bare soils generally fall below 0.2. In contrast, even sparse or water-stressed vegetation commonly produces NDVI values exceeding 0.1, validating the use of this cut-off for vegetation classification in heterogeneous urban environments (Zhou et al., 2013; Xue et al., 2024). Following initial segmentation of vegetated areas, individual vegetation objects were classified into four structural categories using LiDAR-derived height thresholds: grass (≤ 0.5 m), bush (> 0.5 m and < 2.5 m), small tree (≥ 2.5 m and < 7 m), and tall tree (≥ 7 m). Such threshold values are widely employed in urban forestry and green infrastructure mapping, as they enable reliable differentiation between vegetation types that may appear spectrally similar in multispectral imagery alone (Li et al., 2012; Casalegno et al., 2017: Gong et al., 2023). Subsequently, the image classification results were merged into a single region, exported as a vector shapefile, and imported into ArcGIS (version 10.8) software for further analysis and visualization.

2.4. Accuracy assessment of green spaces and non-green areas

Classification accuracy was assessed for two land cover classes, green spaces and non-green areas, across three urban catchments characterised by differing levels of land-use intensity: Itä-Pasila (high), Pihlajamäki (intermediate), and Veräjämäki (low). Validation was conducted using the Regional Land Cover reference dataset 2014 provided by the Helsinki Region Environmental Services Authority (HSY, 2014). To support a statistically robust evaluation, 1000 random sampling points were generated independently for each catchment using ArcGIS version 10.8. For each point, corresponding values representing green spaces (1) and non-green areas (0) were extracted from both the classification outputs and the reference dataset. These data were used to construct confusion matrices and calculate six standard accuracy metrics: Overall Accuracy, Kappa Coefficient, User's Accuracy (green space), Producer's Accuracy (green space), User's Accuracy (non-green area), and Producer's Accuracy (non-green area). Together, these metrics offer a comprehensive evaluation of classification accuracy for both land cover classes across different differing levels of land-use intensity urban environments.

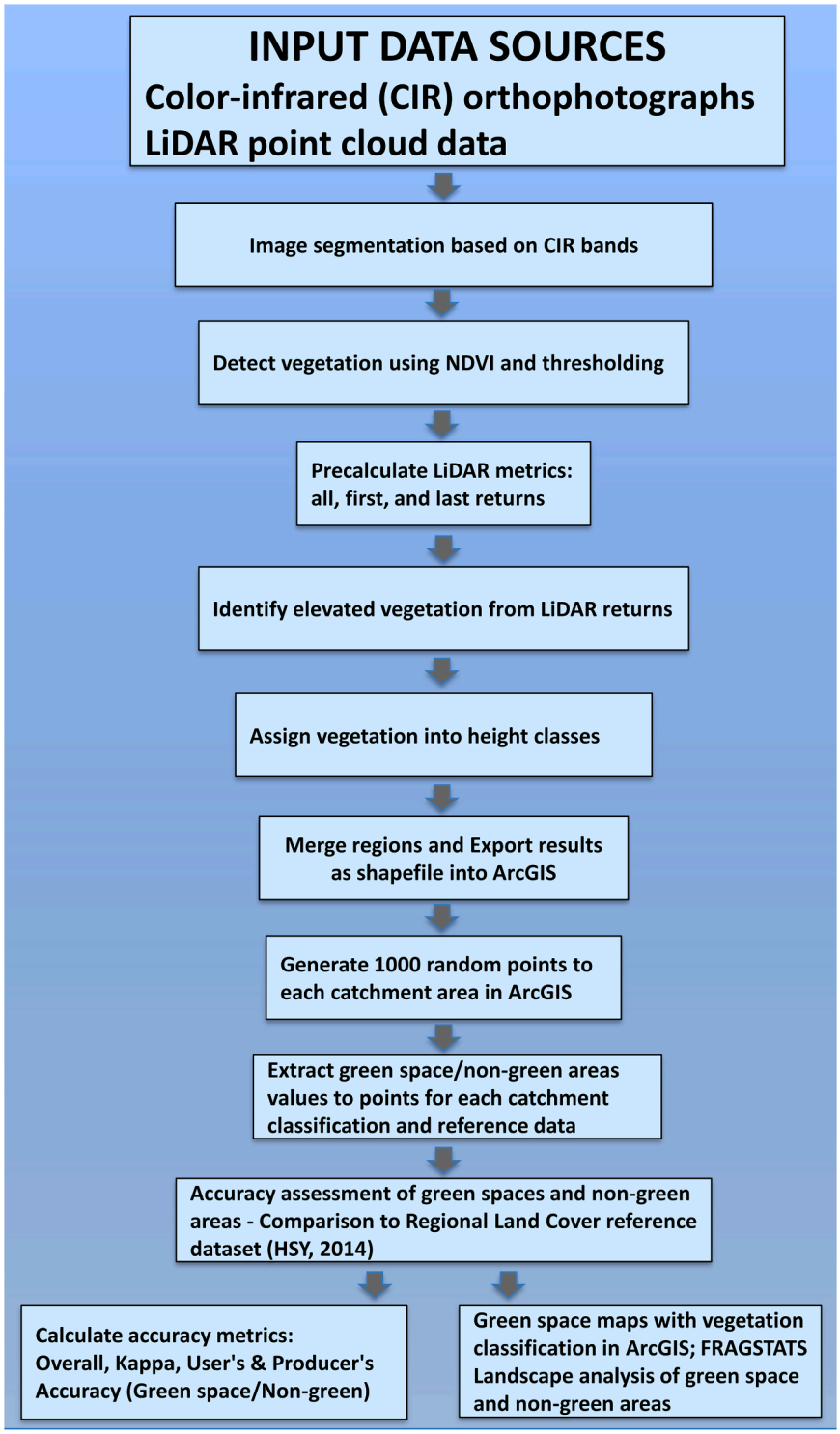

Fig. 3. Flowchart of the green space analysis and mapping processes.

2.5. Map algebra comparison of green spaces and non-green areas with reference data

Classification accuracy for the green space and non-green area maps for three urban catchments were further evaluated with map algebra against HSY reference data with binary raster layers. The analysis was conducted by comparing the classified raster outputs for each cathment to HSY reference raster data set, where pixel values of 1 indicated green

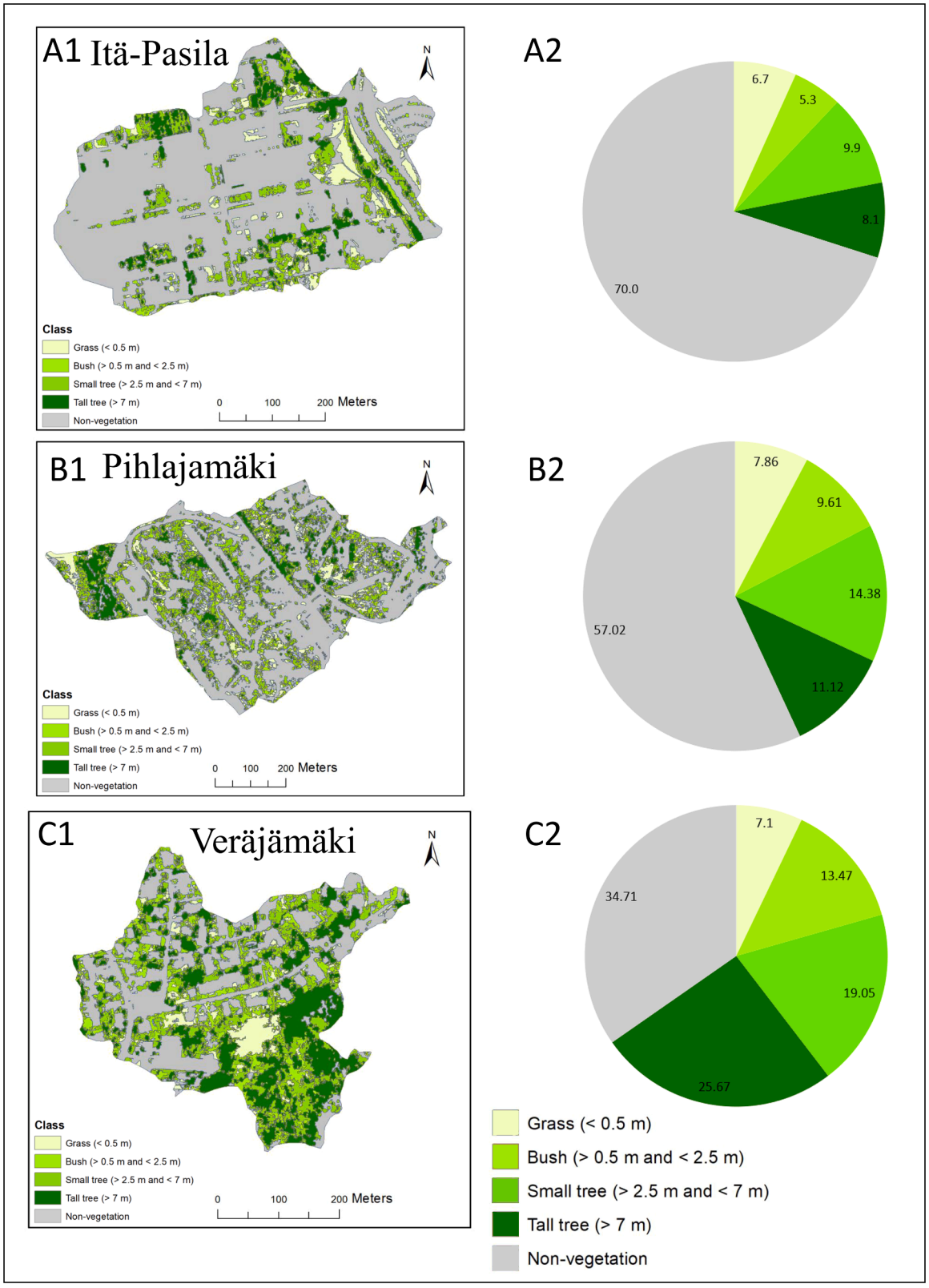

Fig. 4. Green space classification maps (A1, A2 and A3) and areal percentage of green spaces for grass, bush, small trees, tall trees and non-vegetated areas (B1, B2 and B3) of Itä-Pasila, Pihlajamäki and Veräjämäki.

space presence and 0 indicated non-green areas. A difference raster was generated by subtracting the reference raster from the classified raster. This resulted in three possible pixel values: 0 (no difference), 1 (non-green area as green space), and −1 (green space as non-green area).

2.6. Landscape pattern analysis of green spaces and non-green areas

To evaluate the structure and composition of urban green spaces and non-green areas across varying levels of land-use intensity, we analyzed three urban water catchments representing distinct urban forms: Itä-Pasila (urban, high-intensity land-use), Pihlajamäki (residential suburb, intermediate-intensity land-use), and Veräjämäki (peri-urban fringe, low-intensity land-use). We applied a landscape metrics approach using FRAGSTATS v4.3 (McGarigal et al., 2023), a specialized tool for calculating spatial patterns in landscapes. Binary-classified land cover maps were created for each catchment, distinguishing between green space and non-green areas. For each class in every catchment, we computed a suite of 19 class level metrics: Percent of Landscape (PLAND), Number of Patches (NP), Patch Density (PD), Largest Patch Index (LPI), Edge Density (ED), Landscape Shape Index (LSI), Mean, Standard deviation and Coefficient of Variation of Patch Area (AREA_MN; AREA_SD, AREA_CV), ENN_MN (Mean Euclidean Nearest Neighbor Distance), ENN_SD (Standard Deviation of ENN), ENN_CV (Coefficient of Variation of ENN), CLUMPY (Clumpiness Index), PLADJ (Percentage of Like Adjacency), COHESION (Patch Cohesion Index), DIVISION (Landscape Division Index), MESH (Effective Mesh Size), AI (Aggregation Index) and PAFRAC (Perimeter-Area Fractal Dimension). These metrics were chosen for their capacity to quantify spatial heterogeneity, fragmentation, configuration, and connectivity, all of which are critical factors in understanding landscape structure and composition. Additional details on landscape metric definitions and their computational procedures are provided in Supplementary Materials 1. This methodological framework facilitated a systematic evaluation of the spatial patterns of the modelling method versus reference data, enabling a robust assessment of conflict risk classification. Fig. 3 illustrates the proposed method for green space mapping, which integrates vegetation classification based on LiDAR-derived height data with the accuracy assessment of green space and non-green areas, as well as the analysis of landscape metrics.

3. Results

3.1. Vegetation classification results

As expected, Itä-Pasila had the smallest green space coverage (7 ha, 30 %) compared to the other catchments of Pihlajamäki (16.5 ha, 43 %) and Veräjämäki (9.5 ha, 65.5 %) (Fig. 4). In Itä-Pasila, green spaces are fragmented into many small patches and mostly consist of urban parks and individual planted trees. green spaces are planted along the streets which can be easily seen on the classification map (Fig. 4 A1). 70 % is classified as non-vegetation which indicates the urban characteristics of the Itä-Pasila catchment; intense land use, impervious areas, roads, buildings, and parking lots (Fig. 4 A2 and Fig. 2). The northern and southern parts of the catchment are characterized by forest-like urban parks with taller trees. In the middle of the catchment, green spaces are scarce and consist mostly of modest vegetation and grass.

In Pihlajamäki, almost half of the area consists of green spaces. Approximately one quarter is over 7 m high forest. A larger forested area can be seen at the western end of the catchment, but there are also many forest-like lawns within the area (Fig. 4 B1 and B2). Non-vegetated areas consist mostly of roads and tall, long buildings. Additionally, long shadows casted by these buildings increased the amount of classified non-vegetation areas. It is likely that these shadows decrease the classification accuracy. green spaces are fragmented equally around the catchment, only the western side of the catchment consists of a larger patch of continuous forest.

Veräjämäki had the highest proportion (65 %) of green spaces and higher proportion of tall vegetation than the other catchments: more than 25 % of catchment is classified as over 7 m vegetation The southern part of the catchment has a large forest patch consisting of tall trees (Fig. 4 C1). Furthermore, a clear-cutting area from lower to the middle part of the catchment can be distinguished in the classification map as a large patch of < 0.5 m height vegetation. A base rock formation can be seen as non-vegetation area in the northeastern corner of the catchment. green spaces in the northern side of the catchment mostly consist of gardens with some taller trees and short vegetation such as grass and turf. Gardens with tall vegetation were detected in the northern side. A detailed summary of the classification results for each catchment region is provided in Table 1.

3.2. Accuracy assessment of green space and non-green areas across study sites

Green space and non-green area classification performance was evaluated across three urban catchments, reflecting a gradient from high to low land-use intensity. Each site was assessed using six metrics, allowing for a detailed evaluation of classification reliability and consistency (Table 2). Veräjämäki, the least urbanized catchment, delivered the most accurate classification outcomes with an Overall Accuracy of 0.894 and a Kappa of 0.788. green spaces were well captured, with Producer's Accuracy reaching 0.922 and User's Accuracy at 0.873. Similarly, non-green areas showed strong agreement with the reference data, achieving User's Accuracy of 0.917 and Producer's Accuracy of 0.866. Pihlajamäki, representing intermediate land-use intensity, also performed well. The classification achieved an Overall Accuracy of 0.888 and a Kappa of 0.776. Notably, the User's Accuracy for Green areas was the highest among the sites (0.898), suggesting that green spaces in this area were particularly distinguishable. non-green areas also displayed balanced accuracy (User's Accuracy: 0.878; Producer's Accuracy: 0.896). In contrast, Itä-Pasila's more complex and densely built environment posed greater challenges. It recorded the lowest Overall Accuracy (0.859) and Kappa (0.718). While Producer's Accuracy for Green areas remained high (0.920), User's Accuracy dropped to 0.786, indicating difficulties in confidently identifying vegetation at the user level. For non-green areas, high User's Accuracy (0.932) was offset by lower Producer's Accuracy (0.813), reflecting minor under-detection of built-up features.

3.3. Class level landscape patterns for green spaces and non-green areas in three catchment areas

In addition to assessing the classification accuracy of green and non-green vegetation classes across the study catchments, further spatial pattern analysis was conducted to evaluate the structural configuration of the modelled landscapes. Using FRAGSTATS v4.3, a suite of 19 class-level landscape metrics was computed to quantitatively characterise the spatial composition and configuration of green and non-green areas. Each class, green space and non-green space, was evaluated independently across the three catchments using key metrics such as Percent of Landscape (PLAND), Number of Patches (NP), Patch Density (PD), Edge Density (ED), Largest Patch Index (LPI), and others. These metrics offer a robust quantitative basis for understanding the extent, fragmentation, connectivity, and shape complexity of the spatial patterns resulting from the classification models (Table 3).

3.3.1. Itä-Pasila catchment landscape patterns

The Itä-Pasila catchment, characterised by high-density urban development, exhibits a markedly fragmented green space structure. The Percentage of Landscape (PLAND) for green space is only 29.95 %, substantially lower than that of non-green surfaces (70.05 %), indicating green space scarcity in the area. Green patches are numerous but small, as seen in the high Patch Density (PD) of 1143.46 and Number of Patches (NP) of 276, accompanied by a low Mean Patch Area (AREA_MN) of

Table 1
Classification results for the three catchment areas.

Class	Itä-Pasila (ha)	Itä-Pasila (%)	Veräjämäki (ha)	Veräjämäki (%)	Pihlajamäki (ha)	Pihlajamäki (%)
Grass (<= 0.5 m)	1.6	6.7	1.0	7.1	3.0	7.9
Bush (> 0.5 m and < 2.5 m)	1.3	5.3	2.0	13.5	3.7	9.6
Small tree (>= 2.5 m and < 7 m)	2.4	9.9	2.8	19.1	5.5	14.4
Tall tree (>= 7 m)	2.0	8.1	3.7	25.7	4.3	11.1
Non-vegetation	16.9	70.0	5.0	34.7	21.9	57.0
Total	24.1	100.0	14.5	100.0	38.3	100.0

Table 2
Classification accuracy assessment for high (Itä-Pasila), intermediate (Pihlajamäki), and low (Veräjämäki) land-use intensity study catchment sites.

Catchment	Overall Accuracy	Kappa Coefficient	User's Accuracy (Green area)	Producer's Accuracy (Green area)	User's Accuracy (non-green area)	Producer's Accuracy (non-green area)
Itä-Pasila	0.859	0.718	0.786	0.920	0.932	0.813
Pihlajamäki	0.888	0.776	0.898	0.880	0.878	0.896
Veräjämäki	0.894	0.788	0.873	0.922	0.917	0.866

Table 3
FRAGSTATS-based risk class level landscape index analysis for nine metrics classified into four risk classes.

Metric (Full Name)	Itä-Pasila green space	Pihlajamäki green space	Veräjämäki green space	Itä-Pasila non-green	Pihlajamäki non-green	Veräjämäki non-green
PLAND (Percentage of Landscape)	29.95	42.96	65.31	70.05	57.04	34.69
NP (Number of Patches)	276	425	91	59	220	111
PD (Patch Density)	1143.46	1108.62	626.68	244.44	573.87	764.41
LPI (Largest Patch Index)	5.99	10.81	50.20	68.84	52.74	19.50
ED (Edge Density)	888.50	1295.05	1072.65	888.50	1295.05	1072.65
LSI (Landscape Shape Index)	20.96	31.70	14.03	14.15	27.80	18.46
AREA_MN (Mean Patch Area)	0.03	0.04	0.10	0.29	0.10	0.05
AREA_SD (Standard Deviation of Patch Area)	0.12	0.28	0.76	2.14	1.36	0.28
AREA_CV (Coefficient of Variation of Patch Area)	470.60	712.22	731.60	748.28	1368.10	613.67
ENN_MN (Mean Euclidean Nearest Neighbor Distance)	3.92	3.66	3.08	3.99	3.36	4.97
ENN_SD (Standard Deviation of ENN)	4.05	2.61	1.83	2.81	2.44	5.47
ENN_CV (Coefficient of Variation of ENN)	103.29	71.47	59.48	70.52	72.85	110.12
CLUMPY (Clumpiness Index)	0.89	0.87	0.88	0.89	0.87	0.88
PLADJ (Percentage of Like Adjacency)	92.20	92.19	95.44	96.56	94.05	91.77
COHESION (Patch Cohesion Index)	98.04	99.16	99.65	99.93	99.88	99.26
DIVISION (Landscape Division Index)	0.99	0.98	0.74	0.53	0.72	0.96
MESH (Effective Mesh Size)	0.18	0.86	3.71	11.44	10.67	0.61
AI (Aggregation Index)	92.55	92.41	95.75	96.79	94.25	92.18
PAFRAC (Perimeter-Area Fractal Dimension)	1.27	1.32	1.31	1.36	1.36	1.31

0.0262 ha. The Largest Patch Index (LPI) for green space is just 5.99, signifying the absence of a dominant green area. The Landscape Shape Index (LSI) for green is 20.96, which, although higher than non-green, still indicates relatively simple patch shapes. High Edge Density (ED) values (888.50 for both classes) point to complex and fragmented boundaries. The Clumpiness Index (CLUMPY) for green is relatively high (0.8936), yet the Effective Mesh Size (MESH) is very low (0.1816), reflecting poor landscape connectivity. This fragmentation is confirmed by the very high Landscape Division Index (DIVISION) of 0.9925. Connectivity metrics such as Mean Euclidean Nearest Neighbor Distance (ENN_MN) for green space (3.92) and a high ENN_CV (103.29) further indicate isolation among green patches. However, the green space demonstrates moderate aggregation (Aggregation Index (AI) = 92.55), albeit significantly lower than for non-green (96.79).

3.3.2. Pihlajamäki catchment landscape patterns

Pihlajamäki, an intermediate land-use intensity residential area with interspersed forested zones, shows a more balanced distribution between green (42.96 %) and non-green (57.04 %) surfaces. Green areas are considerably more numerous (NP = 425) than in Itä-Pasila, and fragmentation remains high (PD = 1108.62), though green patches are slightly larger on average (AREA_MN = 0.0388 ha). The LPI is 10.81, indicating some presence of dominant green patches, likely reflecting forested segments. Edge complexity is higher in Pihlajamäki than in Itä-Pasila (ED = 1295.05), with complex patch shapes (LSI = 31.70). The Patch Cohesion Index (COHESION) is very high (99.16), implying better structural connectivity despite fragmentation. The DIVISION index is 0.9775 and MESH remains low (0.8612), though significantly higher than in Itä-Pasila. The isolation metric ENN_MN is 3.66, suggesting slightly better proximity between green patches. The PAFRAC value for green patches (1.3173) implies moderate shape complexity. Interestingly, the CLUMPY index is slightly lower than in Itä-Pasila (0.8670), pointing to more disaggregated patch formations.

3.3.3. Veräjämäki catchment landscape patterns

Veräjämäki, a peri-urban or suburban area with lower development intensity, presents the most favourable green space characteristics. Green areas dominate the landscape (PLAND = 65.31 %) compared to non-green (34.69 %). Fragmentation is considerably lower than in the other catchments, evidenced by a lower NP (91) and PD (626.68),

combined with the highest AREA_MN (0.1042 ha) and LPI (50.20), showing the dominance of a single expansive green patch. Spatial cohesion and connectivity are strongest in Veräjämäki, with CLUMPY = 0.8776, AI = 95.75, COHESION = 99.65, and the lowest DIVISION index (0.7444) among the three catchments. The MESH value of 3.71 confirms a less fragmented, more contiguous green landscape. Although ED is moderately high (1072.65), the LSI (14.03) and PAFRAC (1.3144) suggest simpler, less convoluted shapes than in more urbanised zones. ENN_MN (3.08) and ENN_CV (59.48) indicate that patches are not only larger but also more closely located, suggesting improved ecological connectivity.

3.4. Map algebra comparison results

Fig. 5 presents the vegetation classification and validation results for the three study catchments: Itä-Pasila (A), Pihlajamäki (B), and Veräjämäki (C). For each catchment, three panels are displayed: the OBIA-classified vegetation and non-vegetation areas (A1, B1, C1), the corresponding HSY reference datasets (A2, B2, C2), and the resulting difference maps (A3, B3, C3), generated by subtracting the reference raster from the classification output. While visual comparisons between the OBIA classification and the HSY reference data show generally good agreement (Fig. 5 panels 1 and 2), the difference maps offer a more precise representation of spatial mismatches (Fig. 5 panels 1). Notably, the most prominent discrepancies occur in areas where the reference data applied road masks to refine classification accuracy, a step not included in the OBIA–LiDAR framework used in this study. This methodological difference accounts for several areas of disagreement, particularly along road edges. The application of map algebra techniques proves effective in revealing classification inconsistencies that may not be evident through visual or conventional statistical validation alone. These results demonstrate the added value of spatial overlay analysis in enhancing classification assessment and identifying systematic sources of error. A more detailed analysis of these discrepancies, along with their potential causes and implications, is provided in the Discussion section.

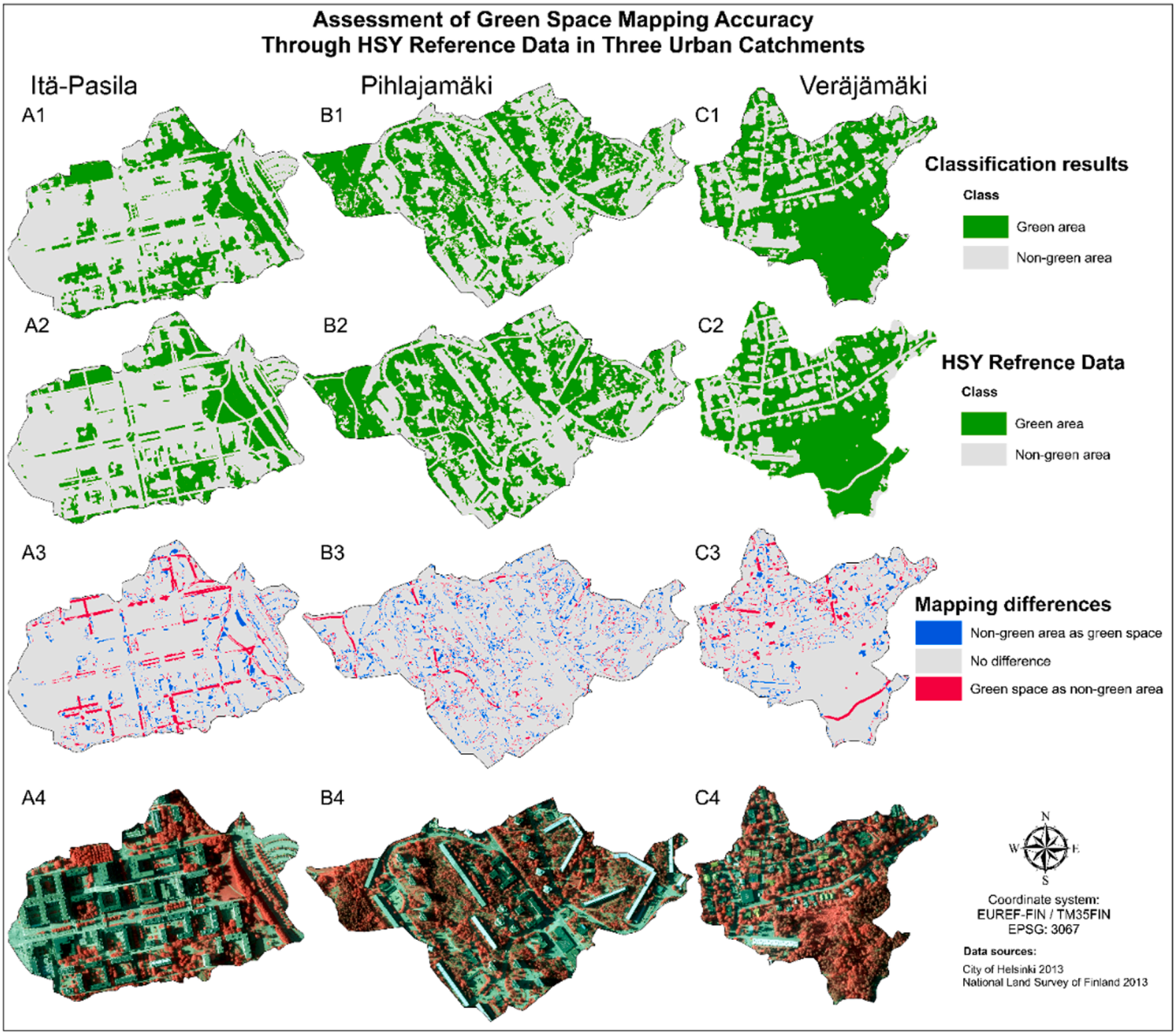

Fig. 5. Validation of OBIA-based binary vegetation classifications (green space and non-green area) against HSY reference data in Itä-Pasila (A), Pihlajamäki (B), and Veräjämäki (C). The figure shows classified outputs (1), reference layers (2), and difference maps (3), and (4) color-infrared (CIR) orthophotographs. Data sources: City of Helsinki, 2013 and Helsinki Region Environmental Services Authority (HSY).

4. Discussion

This study assessed the effectiveness of an OBIA–LiDAR fusion framework for mapping urban green spaces across three Helsinki catchments with varying land-use intensities. The results demonstrate high classification accuracy overall, but reveal challenges in densely built environments where structural complexity and shading reduce the reliability of spectral data.

4.1. Vegetation classification using Object-Based Image Analysis (OBIA) and LiDAR fusion

The object-based classification of vegetation using NDVI thresholds and LiDAR-derived height data proved effective in capturing general patterns of urban greenery, yet varied in performance across urban forms. The stratification into four vegetation height classes added valuable ecological nuance, particularly in distinguishing tree canopy from low-lying vegetation (see Fig. 4.) Veräjämäki displayed the most diverse and evenly distributed vegetation height profile, with a notable presence of high vegetation (≥7 m), which is typical of less densely built urban peripheries (Fig. 4 C1 and C2). By contrast, Itä-Pasila's green space was dominated by lower vegetation classes (<2.5 m), indicative of landscaped but ecologically simpler environments (Fig. 4 A1 and A2). These differences corroborate prior work indicating that urban density inversely correlates with both the quantity and structural complexity of vegetation (Gill et al., 2007; Strohbach and Haase, 2012). This study highlights the importance of incorporating vegetation height stratification into urban green space mapping, particularly in complex urban environments. By combining OBIA with LiDAR-derived structural data, vegetation was classified into four height categories ranging from less than 0.5 m to greater than or equal to 7 meters. This stratification adds value to spatial pattern analysis by enabling more nuanced interpretations of urban vegetation structure. In the present study, landscape metrics were applied only to a binary classification of green and non-green areas. However, the height-based classification framework provides a strong basis for future analyses of landscape patterns across different urban morphologies. The accuracy of the classification was also evaluated across areas with varying levels of urban intensity, supporting the robustness of the method in heterogeneous settings. Across all three study catchments, green space typologies varied both in area and structural height. Notably, Veräjämäki exhibited the greatest proportion of tall tree cover (≥7 m, 25.7 %), aligning with its higher green space coverage (PLAND = 65.31 %) and lower fragmentation. These findings are consistent with prior research demonstrating that mature urban forests in suburban areas offer superior carbon sequestration, thermal regulation, and ecological habitat (Strohbach and Haase, 2012). Conversely, Itä-Pasila displayed predominantly low vegetation (<2.5 m) and sparse tall trees, further supporting the relationship between land-use intensity and vertical vegetation complexity. The User's Accuracy for green areas was notably low in Itä-Pasila (0.786), likely due to misclassification from building shadows and spectral confusion with impervious surfaces, a common challenge in dense urban typologies (Lu and Weng, 2007). The OBIA approach, when calibrated with LiDAR-derived height thresholds, offered considerable advantages in vertical differentiation of green structures. As other studies have shown, combining spectral and structural metrics significantly improves vegetation class separation and thematic accuracy, especially in multi-layered urban contexts (Nichol and Wong, 2005; Heiden et al., 2012). However, shadow effects, especially from tall buildings in Pihlajamäki and Itä-Pasila, introduced artefacts, increasing non-vegetation misclassification, a limitation also recognised by Ghamisi et al., 2019. In order to further assess the accuracy of the OBIA method in comparison to manual mapping approaches, we conducted a comparative analysis with Lundberg's (2011) study, which evaluated habitat diversity and fragmentation in the same three catchments. Lundberg's methodology involved the manual digitization of green spaces from aerial photographs, in contrast to our vegetation classification mapping approach. As a result, Lundberg's study reported a higher proportion of green spaces and trees for all three catchments, indicating that the method employed in our study may, to some extent, underestimate green space coverage. The most significant disparity was observed in the catchment with intermediate land-use intensity (Pihlajamäki), where Lundberg (2011) recorded a green space proportion 10 % higher and a tree proportion almost 20 % higher. This discrepancy may be attributed to the influence of shadows in the aerial imagery.

4.2. Accuracy assessment of green space and non-green areas across study sites

Classification accuracy varied substantially by catchment, with Veräjämäki achieving the highest agreement with reference data (Overall Accuracy = 0.894; Kappa = 0.788) and Itä-Pasila the lowest (Kappa = 0.718). Higher User's Accuracy for green areas in Veräjämäki (0.936) and Pihlajamäki (0.898) suggests that larger, contiguous green patches facilitated better object delineation and spectral separation. In contrast, the lower accuracy observed in Itä-Pasila is likely due to spectral confusion between built-up surfaces and ornamental vegetation, as well as significant shadowing effects from tall buildings, well-documented challenges in OBIA applications to complex urban environments (Lu and Weng, 2007; Blaschke, 2010). The reliance on NDVI may have further limited detection of sparsely vegetated or heavily shaded areas, as NDVI can underestimate vegetation presence in heterogeneous surfaces (Myint et al., 2011).

4.3. Class-level landscape patterns for green spaces and non-green areas in three catchments

The Itä-Pasila catchment, typified by high land-use intensity and built environments, exhibited the most fragmented and least connected green areas. The landscape metrics for Itä-Pasila highlight a highly fragmented and disaggregated green space structure. Despite a relatively high Patch Density (PD = 1143.46) and Number of Patches (NP = 276), the Largest Patch Index (LPI = 5.99) and Mean Patch Area (AREA_MN = 273.81 m^2) indicate that green spaces are small and spatially dispersed. These patterns are characteristic of highly urbanised areas where impervious surfaces dominate and greenery is relegated to interstitial spaces or ornamental uses (Chiesura, 2004). These findings are consistent also with La Rosa et al. (2014), who emphasise the degrading effects of intense urban fabric on landscape cohesion. Pihlajamäki, characterised by intermediate land-use intensity, presented a more balanced spatial configuration. The green space covered over 50 % of the area, with moderate patch size (AREA_MN = 566.52 m^2) and high Clumpiness (CLUMPY = 0.92). The Aggregation Index (AI = 92.41) and Cohesion (99.16) imply that green areas, while fragmented (NP = 425), remain relatively connected. These results suggest that even in intermediate land-use intensity urban areas, landscape planning, such as the inclusion of adjacent forest stands and open spaces, can foster higher spatial integrity (Haase et al., 2014). The presence of larger vegetated patches and tree clusters is likely responsible for improved landscape metrics and classification accuracy. Pihlajamäki serves as a case in point for how built form typology interacts with green space configuration (Herold et al., 2002). Veräjämäki exhibited the most favourable landscape metrics for green space: a high percentage of landscape (PLAND = 65.31), low fragmentation (PD = 634.06), and substantial Largest Patch Index (LPI = 50.20). These values are indicative of well-preserved or planned natural elements integrated within the suburban fabric. The high Effective Mesh Size (MESH = 3.71) and Clumpiness Index (CLUMPY = 0.88) underscore a structurally robust green space network, conducive to both ecological functioning and recreational uses. This configuration aligns with best-practice urban ecological planning that prioritises patch size, shape, and connectivity for optimal service provision (Tzoulas et al., 2007; Benedict and McMahon, 2006). Moreover,

the high classification accuracy in Veräjämäki confirms the methodological robustness of OBIA when applied to less complex, vegetation-dominated landscapes. These areas serve as critical references for interpreting landscape fragmentation in more urbanised catchments.

4.4. Validation of green and non-green land cover classification against reference landscape metrics

The accuracy of the green space classification was evaluated not only through confusion matrix statistics but also through an in-depth landscape pattern comparison with the Helsinki Region Environmental Services Authority (HSY, 2014) land cover reference dataset. The use of FRAGSTATS metrics enabled a multiscale comparative analysis of landscape structure, patch composition, and spatial configuration. Overall, results suggest that while the OBIA-based green space modelling captured many key structural patterns, the degree of alignment with the reference dataset varied significantly between catchments and land cover classes Table 4.

In Itä-Pasila, the modelled green space (PLAND = 29.95 %) moderately overestimated green area compared to the HSY reference (26.87 %). Despite the relative agreement in total coverage, stark discrepancies emerged in structural metrics. The modelled green space exhibited significantly higher patch density (PD = 1143.46 vs. 932.17) and number of patches (NP = 276 vs. 225), which may be attributed to over-segmentation or misclassification of small vegetated elements such as green roofs or shrubs in shadowed areas, a known limitation in high-density urban environments (Lu and Weng, 2007). This fragmentation is further evidenced by a considerably lower Largest Patch Index (LPI = 5.99 %) in the modelled data than in the reference (2.13 %), suggesting that while many small green patches were captured, fewer large cohesive areas were detected. Landscape Shape Index (LSI) and Edge Density (ED) were relatively consistent between datasets, but mean patch size (AREA_MN) was smaller in the modelled green space, indicating finer-grained and possibly more fragmented outputs. Connectivity-related metrics, such as Clumpiness (CLUMPY = 0.89 vs. 0.90), Aggregation Index (AI = 92.55 vs. 92.42), and Cohesion (98.04 vs. 96.29)—were broadly similar, pointing to some spatial agreement in overall configuration. However, the Division Index (0.993 vs. 0.998) and Effective Mesh Size (MESH = 0.18 vs. 0.046) suggest the modelled green space was somewhat more ecologically connected than the reference, though this may be an artefact of small green patches being treated as individual functional units. Overall, while structural realism is modest, the ecological interpretation of connectivity may be optimistic for this dense urban core.

In the intermediate land-use intensity Pihlajamäki catchment, the classification slightly underestimated green space extent (PLAND = 42.96 % vs. 45.55 %), with a higher number of green patches (NP = 425 vs. 250) and greater patch density (PD = 1108.62 vs. 652.13) than the HSY reference. These discrepancies are likely due to fragmentation induced by shadows, mixed pixels at vegetation edges, and limitations of the NDVI threshold in distinguishing sparse vegetation. Importantly, the modelled data recorded a larger Largest Patch Index (LPI = 10.81 %) than the reference (6.90 %), suggesting some large green elements were more accurately or extensively captured. Edge complexity, as indicated by LSI and ED, was greater in the modelled output (LSI = 31.70 vs. 25.34), consistent with a finer spatial resolution of classified vegetation patches. Connectivity metrics showed higher CLUMPY (0.867 vs. 0.893) and slightly lower Aggregation Index (92.41 vs. 94.16), indicating marginally less spatial cohesion. Nonetheless, Effective Mesh Size (MESH = 0.86 vs. 0.54) and Division Index (0.978 vs. 0.986) suggest slightly higher connectivity in the modelled green space. These values could reflect effective detection of adjacent forest patches or green corridors in OBIA, albeit potentially fragmented into smaller units. Despite these structural differences, spatial aggregation and cohesion in Pihlajamäki were generally comparable between modelled and reference data, supporting the reliability of the model for areas of moderate urban density.

In Veräjämäki low land-use intensity catchment, the modelled green space coverage (PLAND = 65.31 %) closely matched the reference dataset (64.47 %), demonstrating the strongest agreement across all three catchments. The number of patches (NP = 91 vs. 67) and patch

Table 4
Summary of key differences between modelled and reference green space metrics in three urban catchments.

Metric	Catchment	Modelled Value	Reference Value	Key Difference / Observation
PLAND	Itä-Pasila	29.95 %	26.87 %	Slight overestimation; good agreement
	Pihlajamäki	42.96 %	45.55 %	Slight underestimation
	Veräjämäki	65.31 %	64.47 %	Strong agreement
NP	Itä-Pasila	276	225	Over-fragmentation (overdetected patches)
	Pihlajamäki	425	250	Significant over-fragmentation
	Veräjämäki	91	67	Moderate over-fragmentation
PD	Itä-Pasila	1143.46	932.17	Inflated patch density
	Pihlajamäki	1108.62	652.13	Highly inflated density
	Veräjämäki	626.68	461.4	Mild inflation
LPI	Itä-Pasila	5.99	2.13	Larger dominant patch detected than actual
	Pihlajamäki	10.81	6.9	Over-dominance in model
	Veräjämäki	50.2	30.26	Strong overestimation of patch dominance
ENN_MN	Itä-Pasila	3.92	5.62	Underestimated inter-patch distance
	Pihlajamäki	3.66	4.52	Underestimated
	Veräjämäki	3.08	4.17	Underestimated
COHESION	Itä-Pasila	98.04	96.29	Close agreement; slightly higher cohesion in model
	Pihlajamäki	99.16	98.88	Good agreement
	Veräjämäki	99.65	99.19	Excellent match
DIVISION	Itä-Pasila	0.993	0.998	Lower division → model shows less fragmentation
	Pihlajamäki	0.978	0.986	Model detects slightly more connected landscape
	Veräjämäki	0.744	0.893	Model underestimates fragmentation significantly
MESH	Itä-Pasila	0.18	0.046	Larger effective mesh in model (false continuity)
	Pihlajamäki	0.86	0.54	Moderate overestimation
	Veräjämäki	3.71	1.55	Strong overestimation of connectivity
CLUMPY	All	~0.87–0.89	~0.89–0.90	Good agreement across all catchments
AREA_CV	Itä-Pasila	470.6	221.1	Much higher variation → noisy classification
	Pihlajamäki	712.22	400.24	Strong over-fragmentation
	Veräjämäki	731.6	402.51	Over-fragmentation evident

density (PD = 626.68 vs. 461.40) were also much closer, indicating lower segmentation errors. The modelled Largest Patch Index (LPI = 50.20 %) significantly exceeded that of the reference (30.26 %), suggesting that major green infrastructure was not only captured but possibly overgeneralised into fewer, larger entities, perhaps due to spectral homogeneity in extensive vegetated areas. Edge Density (ED) and Shape Index (LSI) were also similar, confirming consistency in spatial delineation. Connectivity metrics were particularly strong in Veräjämäki: modelled green space showed a higher MESH (3.71 vs. 1.55), lower Division Index (0.744 vs. 0.893), and comparable CLUMPY and AI values. These results indicate that the OBIA approach was effective in preserving the spatial continuity and functional connectivity of green networks in suburban settings. The high congruence between modelled and reference datasets in Veräjämäki supports the robustness of the classification method in low-density areas with larger and more cohesive green patches, conditions that favour object-based analysis due to lower spectral noise and clearer boundary definition.

4.5. Map algebra comparison

The map algebraic difference raster analysis revealed spatially explicit discrepancies between OBIA-derived green space and the Helsinki Region Environmental Services (HSY) reference data (Fig. 5). The greatest discrepancies were observed at the boundaries of vegetation patches, in shadowed areas, and along narrow linear features such as hedges and grass strips. A key source of disagreement stems from differences in preprocessing: the reference dataset employs road masks to refine classification accuracy, whereas the OBIA–LiDAR framework developed in this study does not incorporate such masking. These discrepancies are especially prominent along road edges. To improve future classification outcomes, it is recommended to integrate available ancillary masks, such as those for roads, buildings, rocky outcrops, and bogs, into the classification workflow. In Itä-Pasila, misclassification was pronounced in densely built zones with artificial landscaping, likely due to spectral mixing and height ambiguity. These errors are consistent with known limitations of NDVI in capturing vegetation under complex lighting and structural conditions (Heiden et al., 2012). By contrast, in Veräjämäki, disagreement was largely constrained to edge pixels, suggesting better alignment with HSY datasets. While map algebra offers an intuitive and powerful means for visualising agreement, it is sensitive to positional mismatches and registration errors. Small geometric offsets can produce exaggerated difference zones. Therefore, its use is best complemented by statistical validation.

4.6. Interpretation and implications

These findings indicate that land-use intensity has a strong influence on green space structure. Highly urbanised Itä-Pasila is dominated by fragmented, isolated green patches, while Pihlajamäki represents a transitional form with improved but still limited cohesion. In contrast, Veräjämäki demonstrates a more continuous and dominant green infrastructure with better spatial connectivity. These structural variations are not merely aesthetic but critically influence urban biodiversity, ecosystem service delivery, and climate adaptation capacity. The implications are particularly salient for urban planning and green infrastructure policy.

4.7. Study limitations

Firstly, LiDAR data tends to underestimate tree heights, as the signal may not reach the highest point of a tree, or in some cases, the signal may not be strong enough to produce a detectable echo (Yu et al., 2004). Additionally, dense vegetation beneath the canopy layer may lead to an overestimation of the digital terrain model (DTM), consequently resulting in an overestimation of the canopy height model (Holopainen et al., 2013). Various factors can contribute to the underestimation of vegetation height, including the choice of algorithm for digital terrain- and canopy height model generation, the extent and height of undergrowth, the algorithm for digital terrain model calculation, laser system sensitivity, signal processing thresholding algorithms, pulse penetration into the canopy, and the shape and species of trees (Holopainen et al., 2013).

Secondly, the presence of shadows significantly affected the accuracy of green space classification. This challenge has been reported in previous studies (Dare, 2005; Degerickx et al., 2020; Zylshal et al., 2016), as shadows represent one of the most common sources of error in remotely sensed data. Objects cast in shadows experience partial or complete spectral information loss (Dare, 2005), rendering the calculation of the normalized difference vegetation index (NDVI) to identify live vegetation impossible for these objects. Numerous green spaces were incorrectly identified as non-vegetation due to shadow effects. This issue was particularly prominent in the Pihlajamäki and Itä-Itä-Pasila catchments (Fig. 6A) due to the abundance of tall buildings that cast shadows over green areas. In contrast, Veräjämäki demonstrated a higher classification accuracy of 92 %, which can be attributed to less intense land use and the absence of tall buildings. Low-rise apartments in Veräjämäki did not pose the same challenges as the taller buildings. The occurrence of shadows is influenced by two main factors: the number of elevated objects and the time of image capture. The time of capture determines the angle of incoming sunlight and the length of shadows cast by elevated objects. While the exact capture time of the aerial images was unknown, aerial surveys in Finland are typically conducted during spring, and the angle and length of shadows in our imagery suggest late afternoon capture, which likely contributed to the reduced classification accuracy. Therefore, for improved green space detection and classification, it is recommended to capture images at midday. Introducing a mechanism to address shaded green spaces could enhance classification accuracy in modelling. Several attempts have been made to tackle the shadow issue, but recovering and restoring shadow-covered information from very high-resolution imagery in urban areas has proven challenging (Dare, 2005). For example, Zhou et al. (2009) applied object-based techniques to evaluate three alternative algorithms for classifying shaded areas in high spatial resolution urban imagery. The most successful approach for shadow classification involved multisource data fusion using two different images. However, as noted by Zhou et al. (2009) and Dare (2005), using multisource data fusion on high spatial resolution images can be problematic due to radiometric disparities and spatial misalignment between distinct images, which can result in significant inaccuracies. One alternative solution, as suggested by Degerickx et al. (2020), involves collecting additional training data specifically for shadow classification. This data could be integrated with existing training data or used to train a separate model dedicated to shadow classification. In our study, there were instances of minor non-vegetation objects being incorrectly classified as green spaces. For example, individual streetlamps were erroneously identified as elevated vegetation when surrounded by grass lawns (Fig. 6B). This misclassification may be attributed to suboptimal segmentation parameters, specifically the scale parameter that determines the size of objects generated during the segmentation process. A higher scale setting might have prevented the classification of smaller elements. Previous research has documented this issue, as noted by Chen et al. (2018), who reported mis-segmentation of object boundaries during image segmentation, which led to the improper amalgamation of small land cover patches into neighboring objects. Although these cases generally encompass very small areas, their impact on overall accuracy is likely minimal. Several classification errors were observed in non-vegetated areas, particularly where building roofs were misclassified as green spaces (Fig. 6C). This effect was more pronounced in areas characterized by low land-use intensity, where some building roofs exhibited a reddish hue. These roofs displayed spectral properties resembling vegetation, causing them to exceed the NDVI threshold and be wrongly categorized as vegetation. Similar issues were noted

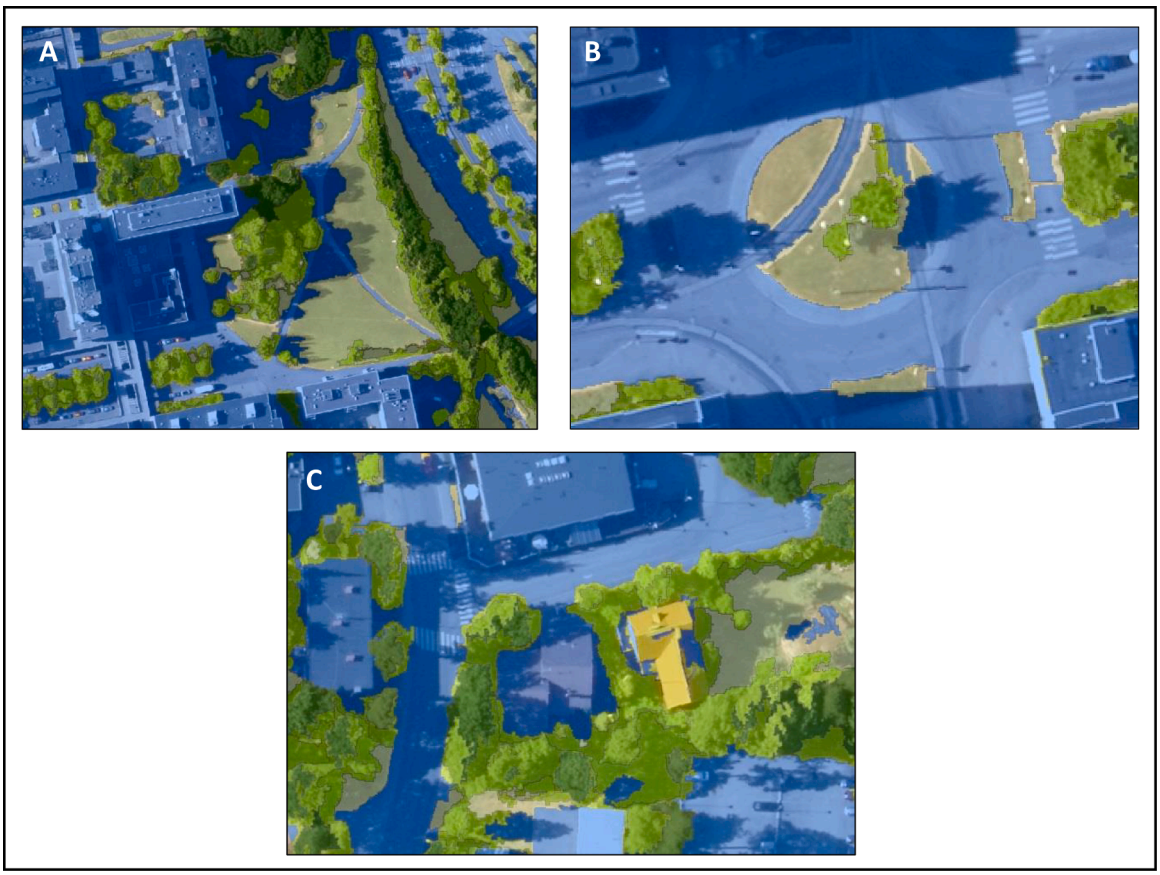

Fig. 6. Illustration of classification errors: shaded objects (A); Mixed object (B) and color confusion (C). Green indicates actual green spaces, blue represents non-vegetated areas, and yellow highlights building roofs that were misclassified as green spaces. Data source: City of Helsinki, 2013.

regarding red cars on the streets of Itä-Pasila. The problem could potentially be mitigated by adjusting the NDVI threshold value; however, this adjustment may result in the exclusion of true green areas from the classification. An alternative method for reducing erroneous classifications due to building roofs would involve the pre-filtering of buildings before the classification process. For instance, Nahhas et al. (2018) employed a deep learning technique to identify buildings using LiDAR-orthophoto fusion, obviating the need for modification of NDVI threshold levels. Overall, deep learning techniques has proven to be valuable new methodology for very high-resolution urban data classification (see Audebert et al., 2018), however, most resent advancers have integrated deep learning techniques into object based image analysis (OBIA), and according to Ma et al. (2024), its full potential remains largely unexplored and thus it should studied in more detail in future.

5. Conclusions

This study assessed the applicability of a hybrid OBIA–LiDAR methodology for mapping urban green spaces in three Helsinki catchments representing varying levels of land-use intensity. The findings underscore the importance of integrating spectral and structural data for detailed urban vegetation classification, particularly where vertical vegetation complexity influences ecological service delivery.

Vegetation height stratification into four classes provided critical ecological granularity. Veräjämäki, a low-density suburban catchment, demonstrated the highest classification accuracy (Overall Accuracy = 0.894), substantial tall tree cover (≥7 m), and high spatial cohesion. This supports the notion that OBIA performs optimally in less fragmented, vegetation-dominated landscapes. In contrast, Itä-Pasila's high-density urban core posed significant challenges, including NDVI limitations, spectral confusion with impervious surfaces, and extensive shadow effects from tall buildings, leading to the lowest classification accuracy.

The landscape metrics confirmed a clear gradient in green space fragmentation and connectivity, correlating with land-use intensity. The OBIA–LiDAR approach proved capable of detecting patch-level structural variation and continuity across urban forms. Veräjämäki's landscape showed high connectivity and low fragmentation, while Pihlajamäki exhibited intermediate spatial cohesion. Itä-Pasila featured fragmented and spatially disaggregated green patches, characteristic of highly urbanised environments. Validation against Regional Land Cover reference dataset 2014 provided by the Helsinki Region Environmental Services Authority (HSY) and map algebra comparison confirmed general alignment in spatial structure, especially in suburban catchments. However, discrepancies in patch count, shape, and classification at shadowed boundaries highlight the need for improved segmentation tuning, shadow compensation, and multi-source data fusion. Misclassification of elevated non-vegetation features such as rooftops and light poles also emphasises the value of pre-classification filtering techniques.

In conclusion, the OBIA–LiDAR fusion framework provides a robust, scalable approach to urban green space mapping, particularly when augmented with vegetation height metrics. However, classification performance remains sensitive to urban form, acquisition timing, and segmentation parameters. Future work should prioritise improving resilience to shadows, integrating deep learning techniques, and enhancing vegetation detection in dense urban settings. This study highlights the practical value of high-resolution green space data for urban planning, especially in rapidly growing cities. The method supports sustainable land-use strategies, green infrastructure enhancement, and urban heat mitigation. Additionally, it enables monitoring of greening policy compliance and identification of areas for restoration or

afforestation. As a transferable workflow, it offers a valuable resource for cities addressing the pressures of rapid urbanisation and environmental change.

CRediT authorship contribution statement

Mika Siljander: Writing – review & editing, Supervision, Methodology, Formal analysis, Data curation, Conceptualization. **Sameli Männistö:** Writing – original draft, Formal analysis. **Kirsi Kuoppamäki:** Writing – review & editing, Supervision, Funding acquisition. **Maija Taka:** Writing – review & editing. **Olli Ruth:** Writing – review & editing, Funding acquisition.

Declaration of Competing Interest

The authors declare that they have no known competing financial interests or personal relationships that could have appeared to influence the work reported in this paper.

Acknowledgements

The authors would like to acknowledge the funding from the Academy of Finland (project URCA, grant number 263308). This work was also supported by the KONE Foundation (grant number 202101976). This study was conducted as part of the Master's Degree Programme in Multidisciplinary Studies on Urban Environmental Issues (MURE) at the University of Helsinki.We also thank the City of Helsinki for the very high-resolution aerial photographs and the National Land Survey of Finland (NLS) for LiDAR data.

The manuscript is original, has not been published elsewhere, and has been approved by all authors. There are no conflicts of interest, and we have acknowledged all funding sources and relevant contributions in the manuscript. We have ensured adherence to ethical research practices and obtained all necessary approvals for the work.

Please address all correspondence concerning author statement to mika.siljander@helsinki.fi

Appendix A. Supporting information

Supplementary data associated with this article can be found in the online version at doi:10.1016/j.ufug.2025.128997.

Data availability

The authors do not have permission to share data.

References

Andersson, E., Barthel, S., Borgström, S., et al., 2019. Reconnecting cities to the biosphere: stewardship of Green infrastructure and urban ecosystem services. AMBIO 43 (2014), 445–453. https://doi.org/10.1007/s13280-014-0506-y.

Alonzo, M., Bookhagen, B., Roberts, D.A., 2014. Urban tree species mapping using hyperspectral and lidar data fusion. Remote Sens. Environ. 148, 70–83. https://doi.org/10.1016/j.rse.2014.03.018.

Audebert, N., Le Saux, B., Lefèvre, S., 2018. Beyond RGB: very high resolution urban remote sensing with multimodal deep networks. ISPRS J. Photogramm. Remote Sens. 140, 20–32. https://doi.org/10.1016/j.isprsjprs.2017.05.011.

Benedict, M.A., McMahon, E.T., 2006. Green infrastructure: linking landscapes and communities. Landsc. Ecol. 22, 797–798. https://doi.org/10.1007/s10980-006-9045-7.

Blaschke, T., Lang, S., Lorup, E., Strobl, J., Zeil, P., 2000. Object-oriented image processing in an integrated GIS/remote sensing environment and perspectives for environmental applications. Environ. Inf. Plan. Polit. Public 2, 555–570.

Blaschke, T., 2010. Object based image analysis for remote sensing. ISPRS J. Photogramm. Remote Sens. 65, 2–16. https://doi.org/10.1016/j.

Blaschke, T., Hay, G.J., Kelly, M., Lang, S., Hofmann, P., Addink, E., Queiroz Feitosa, R., van der Meer, F., van der Werff, H., van Coillie, F., Tiede, D., 2014. Geographic Object-Based image analysis - towards a new paradigm. ISPRS J. Photogramm. Remote Sens. 87, 180–191. https://doi.org/10.1016/j.isprsjprs.2013.09.014.

Casalegno, S., Anderson, K., Hancock, S., Gaston, K.J., 2017. Improving models of urban greenspace: from vegetation surface cover to volumetric survey, using waveform laser scanning. Methods Ecol. Evol. 8, 1443–1452. https://doi.org/10.1111/2041-210X.12794.

Cheng, Y., Wang, W., Ren, Z., Zhao, Y., Liao, Y., Ge, Y., Wang, J., He, J., Gu, Y., Wang, Y., Zhang, W., Zhang, C., 2023. Multi-scale feature fusion and transformer network for urban Green space segmentation from high-resolution remote sensing images. Int. J. Appl. Earth Obs. Geoinf.

Chen, Y., Zhou, Y., Ge, Y., An, R., Chen, Yu, 2018. Enhancing land cover mapping through integration of pixel-based and object-based classifications from remotely sensed imagery. Remote Sens. 10. https://doi.org/10.3390/rs10010077.

Chiesura, A., 2004. The role of urban parks for the sustainable city. Landsc. Urban Plan. 68 (1), 129–138. https://doi.org/10.1016/j.landurbplan.2003.08.003.

Dare, P.M., 2005. Shadow analysis in high-resolution satellite imagery of urban areas. Photogramm. Eng. Remote Sens. 71, 169–177. https://doi.org/10.14358/PERS.71.2.169.

Degerickx, J., Hermy, M., Somers, B., 2020. Mapping functional urban Green types using high resolution remote sensing data. Sustain 12, 1–35. https://doi.org/10.3390/su12052144.

Derkzen, M.L., van Teeffelen, A.J.A., Verburg, P.H., 2015. REVIEW: quantifying urban ecosystem services based on high-resolution data of urban Green space: an assessment for rotterdam, the Netherlands. J. Appl. Ecol. 52, 1020–1032. https://doi.org/10.1111/1365-2664.12469.

Elmqvist, T., Setälä, H., Handel, S.N., van der Ploeg, S., Aronson, J., Blignaut, J.N., Gómez-Baggethun, E., Nowak, D.J., Kronenberg, J., de Groot, R., 2015. Benefits of restoring ecosystem services in urban areas. Curr. Opin. Environ. Sustain 14, 101–108. https://doi.org/10.1016/j.cosust.2015.05.001.

European Environment Agency (EEA) 2016. Urban Atlas: Land Cover / Land Use Data for 2012. European Union, Copernicus Land Monitoring Service. ⟨https://land.copernicus.eu/local/urban-atlas⟩.

Flanders, D., Hall-Beyer, M., Pereverzoff, J., 2003. Preliminary evaluation of ecognition object-based software for cut block delineation and feature extraction. Can. J. Remote Sens. 29, 441–452. https://doi.org/10.5589/m03-006.

Ghamisi, P., Yokoya, N., Li, J., Liao, W., Liu, S., Plaza, J., Rasti, B., Plaza, A., 2019. Multisource and multitemporal data fusion in remote sensing: a comprehensive review of the state of the art. IEEE Geosci. Remote Sens. Mag. 7 (1), 6–39. https://doi.org/10.1109/MGRS.2018.2890023.

Gausman, H.W. (1977). Reflectance of leaf components, Remote Sens. Environ. 6(1) (1–9). https://doi.org/10.1016/0034-4257(77)90015-3.

Georganos, S., Grippa, T., Vanhuysse, S., Lennert, M., Shimoni, M., Wolff, E., 2018. Very high resolution Object-Based land Use-Land cover urban classification using extreme gradient boosting. IEEE Geosci. Remote Sens. Lett. 15, 607–611. https://doi.org/10.1109/LGRS.2018.2803259.

Gill, S.E., Handley, J.F., Ennos, A.R., Pauleit, S., 2007. Adapting cities for climate change: the role of the Green infrastructure. Built Environ. 33 (1), 115–133. https://doi.org/10.2148/benv.33.1.115.

Goldshleger, N., Shoshany, M., Karnibad, L., Arbel, S., Getker, M., 2009. Generalising relationships between runoff-rainfall coefficients and impervious areas: an integration of data from case studies in Israel with data sets from Australia and the USA. Urban Water J. 6, 201–208. https://doi.org/10.1080/15730620802246355.

Gong, Y., Li, X., Du, H., Zhou, G., Mao, F., Zhou, L., Zhang, B., Xuan, J., Zhu, D., 2023. Tree species classifications of urban forests using UAV-LiDAR intensity frequency data. Remote Sens. 15 (1), 110. https://doi.org/10.3390/rs15010110.

GTK 2015. Superficial deposits 1:20,000 / 1:50,000 [data]. Geological Survey of Finland (GTK). http://hakku.gtk.fi (accessed 9. June 2025).

Gunawardena, K.R., Wells, M.J., Kershaw, T., 2017. Utilising Green and bluespace to mitigate urban heat island intensity. Sci. Total Environ. 584–585. https://doi.org/10.1016/j.scitotenv.2017.01.158.

Gülçin, D., Akpınar, A., 2018. Mapping urban Green spaces based on an Object-Oriented approach. Bilge Int. J. Sci. Technol. Res. 2, 71–81. https://doi.org/10.30516/bilgesci.486893.

Haase, D., Larondelle, N., Andersson, E., et al., 2014. A quantitative review of urban ecosystem service assessments: concepts, models, and implementation. AMBIO 43, 413–433. https://doi.org/10.1007/s13280-014-0504-0.

Heiden, U., Heldens, W., Roessner, S., Segl, K., Esch, T., Mueller, A., 2012. Urban structure type characterization using hyperspectral remote sensing and height information. Landsc. Urban Plan. 105 (4), 361–375. https://doi.org/10.1016/j.landurbplan.2012.01.001.

Helsinki Region Environmental Services Authority (HSY), 2014. Regional Land Cover dataset. Available at: https://www.hsy.fi/en/.

Herold, M., Scepan, J., Clarke, K.C., 2002. The Use of Remote Sensing and Landscape Metrics to Describe Structures and Changes in Urban Land Uses. Environment and Planning A: Economy and Space, 34(8), 1443-1458. https://doi.org/10.1068/a3496 (Original work published 2002).

Hidalgo García, D., 2023. Spatio-temporal analysis of the urban Green infrastructure of the city of granada (Spain) as a heat mitigation measure using high-resolution images sentinel 3. Urban For. Urban Green. 87, 128061.

Holopainen, M., Hyyppä, J., Vastaranta, M., 2013. Laserkeilaus metsävarojen hallinnassa. Hels. Yliop. Mets. ätieteiden Laitok. Julk. 5, 1–75.

Hu, X., Xu, C., Chen, J., Lin, Y., Lin, S., Wu, Z., Qiu, R., 2022. A synthetic landscape metric to evaluate urban vegetation quality: a case of fuzhou city in China. Forests 13 (7), 1002. https://doi.org/10.3390/f13071002.

Jin, H., Mountrakis, G., 2022. Fusion of optical, radar and waveform LiDAR observations for land cover classification. ISPRS J. Photogramm. Remote Sens. 187, 171–190.

Kuras, A., Brell, M., Rizzi, J., Burud, I., 2021. Hyperspectral and lidar data applied to the urban land cover machine learning and neural-network-based classification: a review. Remote Sens. 13 (17), 3393.

La Rosa, D., Spyra, M., Inostroza, L., 2014. Indicators of cultural ecosystem services for urban planning: a review. Ecol. Indic. 61 (1), 74–89. https://doi.org/10.1016/j.ecolind.2015.04.028.

Lehmann, I., Mathey, J., Rößler, S., Bräuer, A., Goldberg, V., 2014. Urban vegetation structure types as a methodological approach for identifying ecosystem services - application to the analysis of micro-climatic effects. Ecol. Indic. 42, 58–72. https://doi.org/10.1016/j.ecolind.2014.02.036.

Li, W., Guo, Q., Jakubowski, M.K., Kelly, M., 2012. A new method for segmenting individual trees from the lidar point cloud. Photogramm. Eng. Remote Sens. 78 (1), 75–84. https://doi.org/10.14358/PERS.78.1.75.

Lu, D., Weng, Q., 2007. A survey of image classification methods and techniques for improving classification performance. Int. J. Remote Sens. 28 (5), 823–870. https://doi.org/10.1080/01431160600746456.

Lundberg, P., 2011. Elinympäristöjen monimuotoisuus ja pirstoutuneisuus kaupungistumisasteeltaan erilaisilla valuma-alueilla helsingissä ja lahdessa - sivuaineen pro gradu. Unpublished Msc Thesis. University of Helsinki.

Ma, L., Li, M., Zhang, X., Liu, Y., Li, D., 2024. Deep learning meets object-based image analysis: tasks, challenges, strategies, and perspectives. IEEE Geosci. Remote Sens. Mag. https://doi.org/10.1109/MGRS.2024.3489952.

Man, Q., Dong, P., Yang, X., Wu, Q., Han, R., 2020. Automatic extraction of grasses and individual trees in urban areas based on airborne hyperspectral and LiDAR data. Remote Sens. 12 (17), 2725.

Mathieu, R., Freeman, C., Aryal, J., 2007. Mapping private gardens in urban areas using object-oriented techniques and very high-resolution satellite imagery. Landsc. Urban Plan 81, 179–192. https://doi.org/10.1016/j.landurbplan.2006.11.009.

McGarigal, K., S.A., Cushman, Ene, E., 2023. FRAGSTATS v4: Spatial Pattern Analysis Program for Categorical Maps. Computer software program produced by the authors; available at the following web site: ⟨https://www.fragstats.org⟩.

McGaughey, R.J., 2024. FUSION/LDV: Software for LIDAR Data Analysis and Visualization. USDA Forest Service, Pacific Northwest Research Station. Available at: http://forsys.cfr.washington.edu/software/fusion/FUSION_manual.pdf (Accessed 9 June 2025).

Megahed, Y., Shaker, A., Yan, W.Y., 2021. Fusion of airborne LiDAR point clouds and aerial images for heterogeneous land-use urban mapping. Remote Sens. 13 (4), 814.

Myint, S.W., Gober, P., Brazel, A., Grossman-Clarke, S., Weng, Q., 2011. Per-pixel vs. Object-based classification of urban land cover extraction using high spatial resolution imagery. Remote Sens. Environ. 115 (5), 1145–1161. https://doi.org/10.1016/j.rse.2010.12.017.

Nahhas, F.H., Shafri, H.Z.M., Sameen, M.I., Pradhan, B., Mansor, S., 2018. Deep learning approach for building detection using LiDAR-Orthophoto fusion. J. Sens. 2018. https://doi.org/10.1155/2018/7212307.

Nichol, J.E., Wong, M.S., 2005. Modeling urban environmental quality in a tropical city. Landsc. Urban Plan. 73 (1), 49–58. https://doi.org/10.1016/j.landurbplan.2004.08.004.

Parmehr, E.G., Amati, M., Fraser, C.S., 2016. Mapping urban tree canopy cover using fused airborne lidar and satellite imagery data. ISPRS Ann. Photogramm. Remote Sens. Spat. Inf. Sci. 3, 181–186.

Pfleiderer, P., Schleussner, C.-F., Kornhuber, K., Coumou, F., 2019. Summer weather becomes more persistent in a 2 °C world. Nat. Clim. Change 9, 666–671. https://doi.org/10.1038/s41558-019-0555-0.

Rouse Jr., J.W., Haas, R.H., Schell, J.A., Deering, D.W., 1973. Monitoring vegetation systems in the great plains with ERTS. Proceedings of the Third Earth Resources Technology Satellite-1 Symposium, pp. 10–14.

Shahtahmassebi, A.R., Li, C., Fan, Y., Wu, Y., Gan, M., Wang, K., Malik, A., Blackburn, G. A., 2021. Remote sensing of urban Green spaces: a review. Urban For. Urban Green. 57, 2–16.

Science, 2016. Rise of the city. 352628810.1126/science.352.6288.906.

Strohbach, M.W., Haase, D., 2012. Above-ground carbon storage by urban trees in Leipzig, Germany: analysis of patterns in a european city. Landsc. Urban Plan. 104 (1), 95–104.

Taka, M., 2012, Maankäytön vaikutus pohjoisten alueiden hulevesiin: esimerkkinä Helsingin kaupunkivaluma-alueet. — Unpublished MSc Thesis. University of Helsinki, Faculty of Science, Department of Geosciences and Geography. ⟨http://urn.fi/URN:NBN:fi-fe2017112251421⟩.

Taka, M., Kokkonen, T., Kuoppamäki, K., Niemi, T., Sillanpää, N., Valtanen, M., Warsta, L., Setälä, H., 2017. Spatio-temporal patterns of major ions in urban stormwater under cold climate. Hydrol. Process. 31, 1564–1577. https://doi.org/10.1002/hyp.11126.

Tong, X., Li, X., Xu, X., Xie, H., Feng, T., Sun, T., Liu, X., 2014. A two-phase classification of urban vegetation using airborne LiDAR data and aerial photography. IEEE J. Sel. Top. Appl. Earth Obs. Remote Sens. 7 (10), 4153–4166.

Tzoulas, K., Korpela, K., Venn, S., Yli-Pelkonen, V., Kaźmierczak, A., Niemelä, J., James, P., 2007. Promoting ecosystem and human health in urban areas using Green infrastructure: a literature review. Landsc. Urban Plan. 81 (3), 167–178. https://doi.org/10.1016/j.landurbplan.2007.02.001.

United Nations, 2022. Sustainable Development Goals Report 2022. United Nations Department of Economic and Social Affairs, New York. Available at: https://unstats.un.org/sdgs/report/2023/Goal-11/ [Accessed 19 June 2025].

Ward Thompson, C., Roe, J., Aspinall, P., Mitchell, R., Clow, A., Miller, D., 2012. More Green space is linked to less stress in deprived communities: evidence from salivary cortisol patterns. Landsc. Urban Plan 105, 221–229. https://doi.org/10.1016/j.landurbplan.2011.12.01.

Wolff, F., Kolari, T.H.M., Villoslada, M., Tahvanainen, T., Korpelainen, P., Zamboni, P.A. P., Kumpula, T., 2023. RGB vs. Multispectral imagery: mapping aapa mire plant communities with UAVs. Ecol. Indic. 148, 110140. https://doi.org/10.1016/j.ecolind.2023.110140.

Voogt, J.A., Oke, T.R., 2003. Thermal remote sensing of urban climates. Remote Sens. Environ. 86, 370–384. https://doi.org/10.1016/S0034-4257(03)00079-8.

Xiaoxia, S., Jixian, Z., Zhengjun, L., 2005. A comparison of object-oriented and pixel-based classification approaches using quickbird imagery. Chinese Academy of Surveying and Mapping, Beijing, 100039, China.

Xue, J., Zhang, X., Huang, Y., Chen, S., Dai, L., Chen, X., Yu, Q., Ye, S., Shi, Z., 2024. A two-dimensional bare soil separation framework using multi-temporal Sentinel-2 images across China. Int. J. Appl. Earth Obs. Geoinf. 134, 104181. https://doi.org/10.1016/j.jag.2024.104181.

Yan, W.Y., Shaker, A., El-ashmawy, N., 2015. Remote sensing of environment urban land cover classification using airborne LiDAR data: a review. Remote Sens. Environ. 158, 295–310. https://doi.org/10.1016/j.rse.2014.11.001.

Yu, X., Hyyppa, J., Kaartinen, H., Maltamo, M., 2004. Automatic detection of harvested trees and determination of forest growth using airborne laser scanning. Remote Sens. Environ. 90, 451–462. https://doi.org/10.1016/j.rse.2004.02.001.

Zellweger, F., De Frenne, P., Lenoir, J., Rocchini, D., Coomes, D.A., 2019. Advances in microclimate ecology arising from remote sensing. Trends Ecol. Evol. 34 (4), 327–341. https://doi.org/10.1016/j.tree.2018.12.012.

Zhao, C., Pan, Y., Ren, S., Gao, Y., Wu, H., Ma, G., 2024. Accurate vegetation destruction detection using remote sensing imagery based on the three-band difference vegetation index (TBDVI) and dual-temporal detection method. Int. J. Appl. Earth Obs. Geoinf. 127, 103669. https://doi.org/10.1016/j.jag.2024.103669.

Zhang, C., Qiu, F., 2012. Mapping individual tree species in an urban forest using airborne lidar data and hyperspectral imagery. Photogramm. Eng. Remote Sens. 78, 1079–1087. https://doi.org/10.14358/PERS.78.10.1079.

Zhong, Y., Cao, Q., Zhao, J., Ma, A., Zhao, B., Zhang, L., 2017. Optimal decision fusion for urban Land-Use / Land-Cover classification based on adaptive differential evolution using hyperspectral and LiDAR data. Remote Sens. 9. https://doi.org/10.3390/rs9080868.

Zhou, W., 2013. An Object-Based approach for urban land cover classification: integrating LiDAR height and intensity data. IEEE Geosci. Remote Sens. Lett. 10, 928–931. https://doi.org/10.1109/LGRS.2013.2251453.

Zhou, W., Huang, G., Troy, A., Cadenasso, M.L., 2009. Object-based land cover classification of shaded areas in high spatial resolution imagery of urban areas: a comparison study. Remote Sens. Environ. 113, 1769–1777. https://doi.org/10.1016/j.rse.2009.04.007.

Ziter, C., 2016. The biodiversity–ecosystem service relationship in urban areas: a quantitative review. Oikos 125, 761–768. https://doi.org/10.1111/oik.02883.

Zylshal, Z., Sulma, S., Yulianto, F., Nugroho, J.T., 2016. A support vector machine object based image analysis approach on urban Green space extraction using Pleiades-1A imagery. Model. Earth Syst. Environ. 2, 1–12. https://doi.org/10.1007/s40808-016-0108-8.